

---

# Bridge-Tower: Building Bridges Between Encoders in Vision-Language Representation Learning

---

Xiao Xu<sup>1\*</sup>, Chenfei Wu<sup>1\*</sup>, Shachar Rosenman<sup>2</sup>, Vasudev Lal<sup>2</sup>, Nan Duan<sup>1†</sup>

<sup>1</sup>Microsoft Research Asia

<sup>2</sup>Intel Labs, Cognitive Computing Research

{v-xiaoxu1, chewu, nanduan}@microsoft.com,

{shachar.rosenman, vasudev.lal}@intel.com

## Abstract

Vision-Language (VL) models with the TWO-TOWER architecture have dominated visual-language representation learning in recent years. Current VL models either use lightweight uni-modal encoders and learn to extract, align and fuse both modalities simultaneously in a cross-modal encoder, or feed the last-layer uni-modal features directly into the top cross-modal encoder, ignoring the semantic information at the different levels in the deep uni-modal encoders. Both approaches possibly restrict vision-language representation learning and limit model performance. In this paper, we introduce multiple bridge layers that build a connection between the top layers of uni-modal encoders and each layer of the cross-modal encoder. This enables comprehensive bottom-up interactions between visual and textual representations at different semantic levels, resulting in more effective cross-modal alignment and fusion. Our proposed BRIDGE-TOWER, pre-trained with only 4M images, achieves state-of-the-art performance on various downstream vision-language tasks. On the VQAv2 test-std set, BRIDGE-TOWER achieves an accuracy of 78.73%, outperforming the previous state-of-the-art METER model by 1.09% with the same pre-training data and almost no additional parameters and computational cost. Notably, when further scaling the model, BRIDGE-TOWER achieves an accuracy of 81.15%, surpassing models that are pre-trained on orders-of-magnitude larger datasets. Code is available at <https://github.com/microsoft/BridgeTower>.

## 1 Introduction

Vision-Language (VL) tasks aim to perceive, comprehend and fuse both visual and textual information in our complex multi-modal world and then produce cross-modal representation to address difficult cross-modal challenges, such as visual question answering, visual entailment, and image-text retrieval [17, 82, 85]. Recently, by pre-training on large-scale image-text pairs, cross-modal representation has been improved considerably [5, 13, 27, 29, 35, 48, 55, 68, 75, 78, 91]. Many elaborate Vision-Language Pre-training (VLP) objectives are proposed for mining cross-modal knowledge from image-text pairs, such as masked language modeling (MLM) and image-text matching (ITM).

Most existing VL models can be unified into the TWO-TOWER architecture, which consists of a visual encoder, a textual encoder, and a cross-modal encoder. The models differ in the design of the three encoders. Benefiting from the rapid progress and prominent performance of Vision Transformer (ViT) [10] on various vision tasks, recent VL models can adopt ViT as a cross-modal or visual encoder without using region features from heavy and time-consuming pre-trained object detectors.

ViLT [29] adopts linear projection and word embedding as the visual and textual encoders, and uses ViT as the cross-modal encoder to extract, align and fuse the features of both modalities

---

\* Equal contribution. Contribution during Xiao's internship at Microsoft. † Contact Person

simultaneously. While parameter-efficient, it may be difficult for ViLT to learn intra- and cross-modal interactions concurrently. Thus its performance lags behind state-of-the-art performance on downstream VL tasks. METER [13] uses ViT and RoBERTa as the uni-modal encoders and feeds the last-layer uni-modal features directly into the top cross-modal encoder. Although METER achieves performance competitive with the previous region-based state-of-the-art VinVL [91] model, it ignores different levels of semantic information contained in different layers of the uni-modal encoders. This completely overlooks the rich visual and textual semantic knowledge contained in the different layers of the uni-modal encoders. Furthermore, abstract high-level features from uni-modal encoders could be challenging for the top cross-modal encoder to learn cross-modal alignment and fusion [48, 70].

It has been demonstrated that different layers encode different types of information in both vision [10, 14, 50, 57, 88] and language models [26, 43, 54]. Dosovitskiy et al. [10] and Raghu et al. [57] find that lower layers of ViT attend both locally and globally while higher layers primarily incorporate global information. In the upper half of the ViT, most attention heads attend widely across tokens. Jawahar et al. [26] find that the intermediate layers of BERT encode a rich hierarchy of linguistic information, starting with surface features at the bottom, syntactic features in the middle, and then semantic features at the top. Therefore, it makes perfect sense to utilize the features of the different layers to obtain effective improvements in both vision [23, 42, 81, 86, 92] and language [11, 53, 64, 69, 76]. The question, therefore, naturally arises: *can we build a bridge between the different layers of uni-modal encoders and the cross-modal encoder to utilize the multi-layer uni-modal features?*

We propose BRIDGE-TOWER, a novel transformer-based VL model that takes full advantage of the features of different layers in uni-modal encoders. This is achieved by introducing multiple bridge layers for connecting the top layers of uni-modal encoders with each layer of the cross-modal encoder. This enables detailed bottom-up interaction between visual and textual representations at different semantic levels, promoting more effective cross-modal alignment and fusion in the cross-modal encoder. Moreover, in principle, the proposed BRIDGE-TOWER architecture is applicable to any visual, textual or cross-modal encoder.

We conduct extensive experiments on different design choices for BRIDGE-TOWER and fine-tune it on various downstream VL tasks. Experimental results show that with only 4M images for pre-training, our model achieves state-of-the-art performance on various downstream VL tasks, especially 78.73% accuracy on the VQAv2 test-std set, outperforming the previous state-of-the-art METER model by 1.09% with the same pre-training data and almost no additional parameters and computational cost. When further scaling the model, BRIDGE-TOWER achieves 81.15% accuracy on the VQAv2 test-std set, outperforming models that are pre-trained on orders-of-magnitude larger datasets.

Our contributions are threefold:

- We introduce BRIDGE-TOWER, a novel transformer-based VL model that achieves substantial improvements over existing state-of-the-art methods both with and without pre-training.
- We propose using multiple bridge layers to connect the top layers of uni-modal encoders with each layer of the cross-modal encoder. Furthermore, we conduct extensive experiments on different design choices for BRIDGE-TOWER, including the formal definition of bridge layers and the design choices for cross-modal layers.
- We show that BRIDGE-TOWER achieves state-of-the-art results on visual question answering (VQAv2), visual entailment (SNLI-VE), and image-text retrieval (Flickr30K) tasks.

## 2 Related Work

### 2.1 TWO-TOWER Vision-Language Models

Following the taxonomy proposed by ViLT [29], the most recent VL models can be unified into the TWO-TOWER architecture as shown in Figure 1(a)–(d). They feed last-layer representations of the visual and textual encoders into the top cross-modal encoder and can be differentiated by the depth of the textual, visual, and cross-modal encoders.

CLIP [55] and ALIGN [27] are representative models that directly perform a shallow fusion (*e.g.*, dot product) of last-layer representations of equally expressive deep visual and textual encoders in the cross-modal encoder, as illustrated in Figure 1(a). The remaining models perform deep fusion in the multi-layer transformer-based cross-modal encoder but choose uni-modal encoders with varying levels of expressiveness. Numerous works [5, 6, 8, 24, 25, 33, 36, 37, 39, 41, 46, 51, 63, 68, 80,

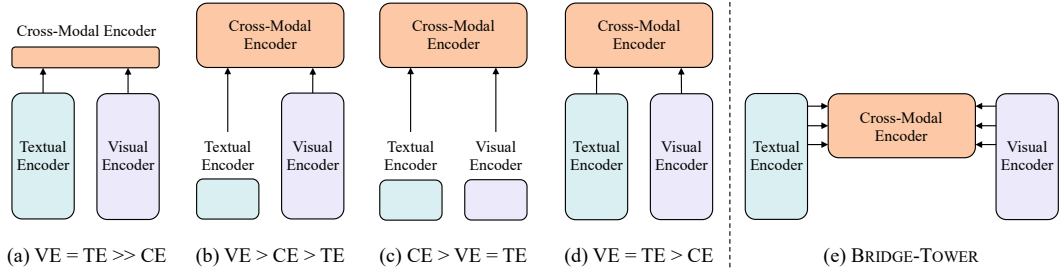


Figure 1: (a)–(d) are four categories of current TWO-TOWER vision-language models; (e) gives a brief illustration of the BRIDGE-TOWER architecture. VE, TE, and CE are short for the Visual Encoder, Textual Encoder, and Cross-modal Encoder, respectively. The height of each rectangle represents its relative computational cost.  $VE = TE$  indicates that the visual encoder and the text encoder have the same or a similar number of parameters or computational costs.

[83, 84, 91, 93] fall in the category of Figure 1(b) as they adopt various types of deep vision models (e.g., Faster R-CNN [58], ResNet [19] or ViT [10]) as their visual encoder to obtain region, grid, or patch features, and concatenate them with word embedding to feed to their top cross-modal encoder. The third category of models [29, 75, 78], illustrated in Figure 1(c), utilizes lightweight visual and lightweight textual encoders and handles both modalities in a single transformer-based cross-modal encoder. In contrast, models [13, 28, 34, 35, 38, 48, 70, 77, 89], which belong to Figure 1(d) category, use expressive deep visual and deep textual encoders and feed their last-layer representation into the top multi-layer cross-modal encoder.

Regardless of the visual, textual, or cross-modal encoder they utilize, most current models ignore the various levels of semantic information in the different layers of the uni-modal encoders, and simply utilize the last-layer uni-modal representations for cross-modal alignment and fusion. While the models belonging to Figure 1(c) appear to retain the possibility of utilizing different levels of uni-modal semantic information, it could be challenging for them to learn intra- and cross-modal interactions concurrently without modality-specific parameters. Their unconstrained cross-modal interaction could impede intra-modal interaction [13, 15]. This may be the reason why the performance of ViLT lags behind models in the Figure 1(d) category, and why SimVLM [78] and OFA [75] need to use significantly more data to obtain competitive performance compared to METER.

Unlike current models, BRIDGE-TOWER, as shown in Figure 1(e), proposes using multiple bridge layers to connect the top layers of uni-modal encoders with each layer of the cross-modal encoder. This does not affect intra-modal interaction, and enables different semantic levels of visual and textual representations to interact thoroughly and mildly in the bottom-up directions. Effective cross-modal alignment and fusion can be achieved at each layer of the cross-modal encoder.

## 2.2 Multi-Layer Feature Utilization

Multi-layer feature utilization has been demonstrated to be an effective method of making full use of the information contained in different layers of the model to improve the representation and generalization capabilities of computer vision [23, 30, 42, 44, 50, 59, 81, 86, 92], natural language processing [1, 3, 11, 12, 26, 53, 64, 69, 76, 79] and multi-modal models [13, 49].

Based on Zeiler and Fergus [88] who show that different patterns are learned in different layers of CNN models, many researchers exploit features of different layers to improve detection and semantic segmentation. U-Net [59] and FPN [42] propose to adopt lateral connections for associating feature maps from different layers across resolutions and semantic levels. The same idea is also applicable to the ViT-based models. SETR [92] and SegFormer [81] aggregate features from different layers in a similar way to FPN, to improve the performance of semantic segmentation.

In natural language processing, researchers [2, 18, 26, 43, 54, 67] find that Recurrent Neural Networks (RNN) [21] and BERT [9] encode different types of semantic information in different layers. Hence, ELMo [53] and Sun et al. [69] use the concatenation or weighted sum of representations from different layers of RNN or BERT as input for different downstream task heads. Dou et al. [11] explore layer aggregation with multi-layer attention mechanisms. Recent multi-modal models also

exploit features from different layers. MBT [49] introduces simple bottleneck tokens at multiple layers to jointly model intra- and restricted cross-modal correlations. While MBT achieves good performance on audio-visual benchmarks, learning complex vision-language alignment and fusion via a limited number of bottleneck tokens instead of a cross-modal encoder is too difficult, which limits the ability of cross-modal alignment. METER [13] feeds the weighted sum of representations from each layer of the bottom uni-modal encoder into the top cross-modal encoder; they find this can improve performance by a small margin without VLP but can degrade performance with VLP.

In a departure from existing models, BRIDGE-TOWER is the first vision-language model to consider detailed interactions between the top layers of uni-modal encoders and each layer of the cross-modal encoder. It is intuitive to connect the uni-modal encoders and the cross-modal encoder via multiple bridge layers, in order to achieve comprehensive and detailed layer-wise interaction between the uni-modal representations of different semantic levels. Most importantly, unlike the simple multi-layer feature fusion method in METER, BRIDGE-TOWER can significantly improve performance both with and without vision-language pre-training on large-scale image-text data.

### 3 Approach

BRIDGE-TOWER consists of a visual encoder, a textual encoder, a cross-modal encoder, and multiple lightweight bridge layers. Our goal is to build a bridge between each uni-modal encoder and the cross-modal encoder to enable comprehensive and detailed interaction at each layer of the cross-modal encoder. Our goal is not to develop new encoders; in principle, one can apply any visual, textual, or cross-modal encoder in the proposed BRIDGE-TOWER architecture.

#### 3.1 Visual Encoder

CLIP [55] has shown its strong capabilities on various computer vision benchmarks. Recent works [13, 63] also demonstrate its great potential for VL tasks. In this paper, we adopt CLIP’s visual encoder, *i.e.*, CLIP-ViT-B/16. For each input 2D image  $\mathbf{I} \in \mathbb{R}^{H \times W \times C}$ , where  $(H, W)$  is the resolution of the input image and  $C$  is the number of channels, ViT [10] reshape it into a sequence of flattened 2D patches  $\mathbf{P} \in \mathbb{R}^{N \times (P^2 C)}$ , where  $(P, P)$  is the image patch resolution and  $N = \frac{HW}{P^2}$  is the number of patches. Similar to BERT [9], ViT also prepends the [class] token to the patch sequence and uses learnable 1D position embeddings  $\mathbf{V}^{pos} \in \mathbb{R}^{(N+1) \times D_v}$ , where  $D_v$  is the dimension of the visual encoder. We can get the input visual representation as:

$$\mathbf{V}_0 = [\mathbf{E}_{[\text{class}]}; \mathbf{p}_1 \mathbf{W}_p; \dots; \mathbf{p}_N \mathbf{W}_p] + \mathbf{V}^{pos}, \mathbf{V}_0 \in \mathbb{R}^{(N+1) \times D_v}, \quad (1)$$

where  $\mathbf{W}_p \in \mathbb{R}^{(P^2 C) \times D_v}$  is the trainable linear projection layer. Each layer of ViT consists of a multi-head self-attention (MSA) block and a feed-forward network (FFN) block. We omit the computation details and simplify them as  $\text{Encoder}_\ell^V$ . The output representation of each layer can then be denoted as  $\mathbf{V}_\ell = \text{Encoder}_\ell^V(\mathbf{V}_{\ell-1}), \ell = 1 \dots L_V$ , where  $L_V$  is the number of layers of the visual encoder.

#### 3.2 Textual Encoder

Since RoBERTa [45] achieves robust performance on a wide range of NLP tasks, we adopt RoBERTa<sub>BASE</sub> as our textual encoder. Each input sequence  $\mathbf{w}$  is tokenized by the byte-level Byte-Pair Encoding (BPE) [56, 61]. [`<s>`] and [`</s>`] are added to the sequence as the start and end tokens, respectively. The input textual representation can be represented as:

$$\mathbf{T}_0 = [\mathbf{E}_{[\text{<s>}]}; \mathbf{E}_{w_1}; \dots; \mathbf{E}_{w_M}; \mathbf{E}_{[\text{</s>}]}] + \mathbf{T}^{pos}, \mathbf{T}_0 \in \mathbb{R}^{(M+2) \times D_t}, \quad (2)$$

where  $\mathbf{E}$  is the word embedding matrix,  $M$  is the number of tokens,  $D_t$  is the dimension of the textual encoder, and  $\mathbf{T}^{pos}$  is the positional embedding matrix. Similarly, we denote each layer of the textual encoder as  $\text{Encoder}_\ell^T$ , and the output representation of each layer can be denoted as  $\mathbf{T}_\ell = \text{Encoder}_\ell^T(\mathbf{T}_{\ell-1}), \ell = 1 \dots L_T$ , where  $L_T$  is the number of layers of the textual encoder.

#### 3.3 Cross-Modal Encoder with Bridge Layers

Hendricks et al. [20] perform analysis on different types of attention mechanisms used in the existing transformer-based cross-modal encoders and demonstrate that the *co-attention* mechanism [48]

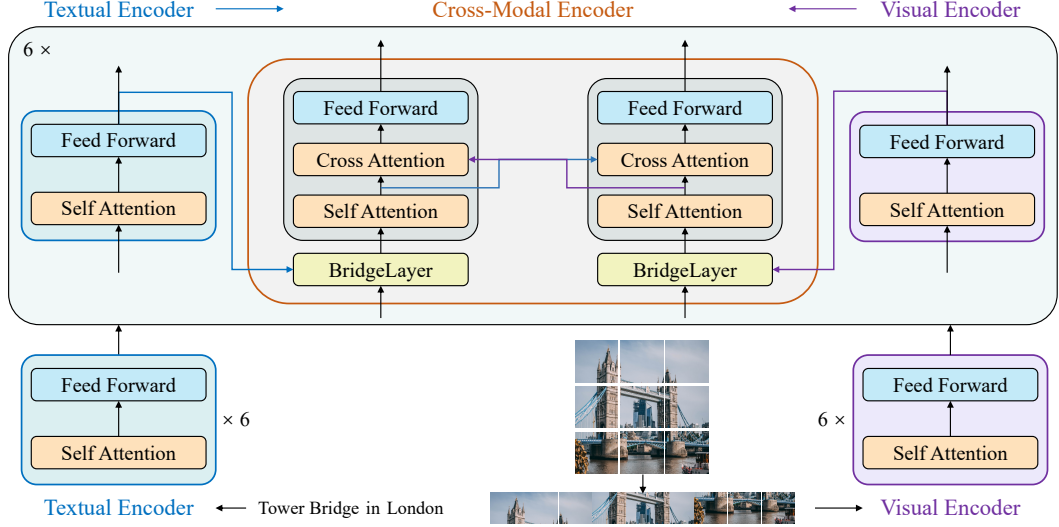


Figure 2: **Illustration of BRIDGE-TOWER.** BRIDGE-TOWER consists of a 12-layer textual encoder, a 12-layer visual encoder, and a 6-layer cross-modal encoder. The top 6 layers of the visual and text encoders are connected to each layer of the cross-modal encoder via bridge layers.

performs best. This mechanism uses a different set of parameters for each modality. For example, for the visual part of the cross-modal encoder, the queries of each MSA block are from the visual modality. However, the keys and values are from the queries of the other modality (*i.e.*, textual). We, therefore, adopt the *co-attention* mechanism. Formally, we define each layer of the cross-modal encoder as  $\text{Encoder}_\ell^Z$ , which consists of a visual part and a textual part. Each part consists of a multi-head self-attention (MSA) block, a multi-head cross-attention (MCA) block, and a feed-forward network (FFN) block. For brevity, the interactions at each layer are defined as:

$$\tilde{\mathbf{Z}}_\ell^V = \mathbf{Z}_{\ell-1}^V, \quad (3)$$

$$\tilde{\mathbf{Z}}_\ell^T = \mathbf{Z}_{\ell-1}^T, \quad (4)$$

$$\mathbf{Z}_\ell^V, \mathbf{Z}_\ell^T = \text{Encoder}_\ell^Z(\tilde{\mathbf{Z}}_\ell^V, \tilde{\mathbf{Z}}_\ell^T), \ell = 1 \dots L_Z, \quad (5)$$

where  $\mathbf{Z}_\ell^{\{V,T\}}$  is the visual or textual part of the cross-modal representation at the  $\ell$ -th layer,  $\tilde{\mathbf{Z}}_\ell^{\{V,T\}}$  is the input of each part, and  $L_Z$  is the number of layers of the cross-modal encoder.

Generally, current VL models, such as METER [13], directly use the representation of the previous layer as the input of  $\text{Encoder}_\ell^Z$  (Equation 3 and 4).  $\mathbf{Z}_0^V, \mathbf{Z}_0^T$  are initialized with the last-layer representations from uni-modal encoders, *i.e.*,  $\mathbf{Z}_0^V = \mathbf{V}_{L_V} \mathbf{W}_V + \mathbf{V}^{type}$ ,  $\mathbf{Z}_0^T = \mathbf{T}_{L_T} \mathbf{W}_T + \mathbf{T}^{type}$ , where  $\mathbf{W}_V \in \mathbb{R}^{D_V \times D_Z}$  and  $\mathbf{W}_T \in \mathbb{R}^{D_T \times D_Z}$  are linear projections,  $\mathbf{V}^{type}$  and  $\mathbf{T}^{type}$  are the visual and textual type embeddings.

However, in this paper, we propose using multiple bridge layers to connect the top layers of uni-modal encoders with each layer of the cross-modal encoder. Bottom-up detailed interaction between visual and textual representations at different semantic levels can be achieved by:

$$\tilde{\mathbf{Z}}_\ell^V = \text{BridgeLayer}_\ell^V(\mathbf{Z}_{\ell-1}^V, \mathbf{V}_j \mathbf{W}_V + \mathbf{V}^{type}), \quad (6)$$

$$\tilde{\mathbf{Z}}_\ell^T = \text{BridgeLayer}_\ell^T(\mathbf{Z}_{\ell-1}^T, \mathbf{T}_k \mathbf{W}_T + \mathbf{T}^{type}), \quad (7)$$

$$\mathbf{Z}_\ell^V, \mathbf{Z}_\ell^T = \text{Encoder}_\ell^Z(\tilde{\mathbf{Z}}_\ell^V, \tilde{\mathbf{Z}}_\ell^T), \quad (8)$$

where  $j \in [1, L_V]$  and  $k \in [1, L_T]$  are the indices of the uni-modal representations of the visual and text encoders. For example, if  $L_V = L_T = 12$  and  $L_Z = 6$ , then to use uni-modal representations of the top 6 layers, we set  $j, k = 7, \dots, 12$ . Utilizing our proposed bridge layers, top-layer uni-modal representations can be bridged with each layer of the cross-modal encoder, thus incorporating different semantic levels of uni-modal representations into cross-modal interaction. In the spirit of ResNet [19] and Transformer [73], we give the simplest formal definition of a bridge layer (*i.e.*, Add&Norm):

$$\text{BridgeLayer}(x, y) = \text{LayerNorm}(x + y). \quad (9)$$

In Section 4.2, we describe the extensive experiments we conducted on different design choices for BRIDGE-TOWER, including the formal definition of bridge layers and the design choices for cross-modal layers.

### 3.4 Pre-training Objectives

We pre-train BRIDGE-TOWER with two commonly used vision-language pre-training objectives: masked language modeling (MLM) and image-text matching (ITM).

**Masked Language Modeling.** MLM is a common choice for language and vision-language pre-training objectives. Given an image-text pair, following UNITER [5], we use conditional masking on MLM, which means we randomly mask 15% of tokens in the token sequence while keeping the input image patch sequence untainted. The model is trained to reconstruct the original tokens conditioned on incomplete input token sequence and complete observed image patch sequence. We adopt the same masking strategy and MLM task head as BERT [9].

**Image-Text Matching.** ITM aims to predict whether the given image-text pair is positive (matched) or negative (not matched). Matched and mismatched image-text pairs are fed into our model with the same probability. We pass the final representation of [class] token and [<s>] token to the non-linear layer activated by Tanh, and feed the concatenation of the output into a linear classifier with cross-entropy loss for binary classification. A similar strategy is also used for downstream tasks.

## 4 Experiment

### 4.1 Implementation Details

The default architecture of BRIDGE-TOWER is shown in Figure 2. BRIDGE-TOWER consists of a pre-trained textual encoder, *i.e.*, RoBERTa<sub>BASE</sub> with 124M parameters, a pre-trained visual encoder, *i.e.*, CLIP-ViT-B/16 with 86M parameters, and a random-initialized 6-layer cross-modal encoder with 113M parameters. For each layer of the cross-modal encoder, the hidden size is set to 768, the intermediate size of feed-forward networks is set to 3,072, and the number of heads is set to 12. The maximum length of the text sequence is set to 50. We use the AdamW [47] optimizer with a base learning rate of  $2e^{-5}$  and weight decay of 0.01. The learning rate is warmed up for 10% of the total training steps and then decayed linearly to zero for the rest of the training steps. Following METER [13], the learning rate of the cross-modal encoder is five times higher than that of the uni-modal encoders. We use an image resolution of  $384 \times 384$  for these downstream VL tasks, except for VQAv2, where we use  $576 \times 576$  for a robust evaluation and comparison. The patch size is  $16 \times 16$ . Center-crop is used to resize each input image to the same resolution, and we also apply RandAugment [7] to the input images following previous work [13, 29, 34, 35].

We evaluate BRIDGE-TOWER by fine-tuning on the visual question answering [17] (VQAv2), visual entailment [82] (SNLI-VE), and image-text retrieval [85] (Flickr30K) tasks. We use the standard settings and splits for all the datasets except for VQAv2, where we follow the common practice [17, 72]: convert VQAv2 to a classification task with 3,129 answer classes; train the model with training data and validation data, and evaluate the model on the test-dev data.

### 4.2 Ablation Study and Analysis

In this section, we focus on different design choices for BRIDGE-TOWER on VQAv2, which is the most popular dataset for VL evaluation. Each model is initialized with CLIP-ViT-B/16 and RoBERTa<sub>BASE</sub>, and then trained without VLP. In our preliminary experiments, the uni-modal representations of the top layers show substantially better performance than the middle and bottom layers. Thus, we use the representation of the top 6 layers of the uni-modal encoders as the corresponding input to each bridge layer in the bottom-up directions.

#### 4.2.1 Design Choice I: Formal Definition of Bridge Layers

Table 1 shows, perhaps unexpectedly but not very surprisingly, that row (a) provides the best results using the minimum number of parameters and achieves an accuracy of 75.18% on the test-dev

Table 1: **Performance and number of parameters for different formal definitions of bridge layers on the VQAv2 dataset.** We omit the layer normalization used in each form.  $x$  denotes the cross-modal representation of the output of the previous layer and  $y$  denotes the input uni-modal representation. The number in parentheses is the difference between it and the best result.

BridgeLayer( $x, y$ )	# Params	Test-Dev
(a) $x + y$	18.4K	<b>75.18</b>
(b) $x \odot y$	18.4K	73.41 (-1.77)
(c) $\alpha x + (1 - \alpha) y, \alpha \in \mathbb{R}^{D_z}$	26.0K	75.08 (-0.10)
(d) $\alpha x + (1 - \alpha) y, \alpha = \sigma(\mathbf{W}[x; y])$	11.8M	75.09 (-0.09)
(e) $\mathbf{W}[x; y]$	11.8M	74.55 (-0.63)
(f) $\mathbf{W}_2(\text{GeLU}(\mathbf{W}_1[x; y]))$	35.4M	74.26 (-0.92)
(g) MCA( $x, y$ )	23.6M	73.67 (-1.51)
(h) FFN(MCA( $x, y$ ))	70.8M	73.54 (-0.64)
(i) $x + y + \mathbf{W}_* [x; y]$	11.8M	75.10 (-0.08)

set of VQAv2. Instead, the additional parameters used for interpolation cause slight performance degradation in rows (c)&(d). Rows (e)–(h) try to incorporate generally used feature transformation forms into the bridge layer, but the additional computation and parameters instead lead to performance degradation. Inspired by ResNet [19] and ViTDet [40], in row (i), we incorporate row (a) into row (e) as the residual connection.  $\mathbf{W}_*$  is initialized as zero so that row (i) is initially equivalent to row (a). Although the performance is significantly higher than row (e) (74.55  $\rightarrow$  75.10), there is no gain compared to row (a). Hence, we choose row (a) (Add&Norm) as the default form of bridge layers.

#### 4.2.2 Design Choice II: Number of Cross-Modal Layers

In BRIDGE-TOWER, the cross-modal encoder is not located on top of the uni-modal encoders, but between them. Each cross-modal layer is connected to one layer of the uni-modal encoder by a bridge layer. Thus, the number of cross-modal layers can be  $[0, 12]$  based on two 12-layer uni-modal encoders. Table 2 shows the performance of BRIDGE-TOWER with different numbers of cross-modal layers. It is illuminating to note that adding more cross-modal layers does not constantly improve performance, possibly because (i) more cross-modal layers are more difficult to train and are more data-hungry; (ii) uni-modal representations of top layers are beneficial to cross-modal alignment and fusion, while uni-modal representations of bottom layers may be less useful and even detrimental.

Table 2: Ablation of the different number of cross-modal layers.

$L_z$	# Params	Test-Dev
0	0.0M	68.21 (-6.97)
2	37.8M	74.12 (-1.06)
4	75.6M	75.00 (-0.18)
6	113.4M	<b>75.18</b>
8	151.2M	75.07 (-0.11)
10	189.0M	75.06 (-0.12)
12	226.8M	74.94 (-0.24)

#### 4.2.3 Design Choice III: Number of Internal and External Cross-Modal Layers

Since the cross-modal layer in the current TWO-TOWER model is on top of the uni-modal encoders, we denote it as the external cross-modal layer, and we denote the cross-modal layer in BRIDGE-TOWER as the internal cross-modal layer. A question naturally arises: *Will performance improve if we use both the internal and external layers?* We fix the total number of cross-modal layers at 6 and study the performance of various combinations of internal and external cross-modal layer numbers. Table 3 shows that the internal layer is more effective than the external layer. This demonstrates that the bridge layer of BRIDGE-TOWER, which connects the top layers of uni-modal encoders with each layer of the cross-modal encoder, can significantly improve performance. Comprehensive and effective layer-wise interactions between uni-modal representations of different semantic levels can be achieved, promoting more effective cross-modal alignment and fusion at each layer of the cross-modal encoder.

Table 3: Ablation of different number of internal and external cross-modal layers. \* denotes multi-layer feature fusion.

# Internal	# External	Test-Dev
6	0	<b>75.18</b>
4	2	75.06 (-0.12)
3	3	74.97 (-0.21)
2	4	74.71 (-0.47)
0	6	74.04 (-1.14)
0	6*	74.52 (-0.66)

We also explore the simple multi-layer feature fusion [13] (last row), where the weighted sum of uni-modal representations of each layer is fed to the top cross-modal encoder. Although it obtains a slightly better performance than the 6 external cross-modal layers (penultimate row, *i.e.*, METER w/o VLP), it is still significantly weaker than the proposed 6 internal cross-modal layers.

Table 4: Comparisons with previous models on visual question answering (VQAv2). The best score is **bolded**. The models are divided into base size and large/huge size.

Model	# Pre-train Images	Use VG-QA For Fine-tuning	Test-Dev		Test-Standard		
			Overall	Yes/No	Number	Other	Overall
ViLT <sub>BASE</sub> [29]	4M	X	71.26	-	-	-	-
UNITER <sub>BASE</sub> [5]	4M	✓	72.70	-	-	-	72.91
VILLA <sub>BASE</sub> [16]	4M	✓	73.59	-	-	-	73.67
UNIMO <sub>BASE</sub> [37]	4M	X	73.79	-	-	-	74.02
ALBEF <sub>BASE</sub> [35]	4M	✓	74.54	-	-	-	74.70
ALBEF <sub>BASE</sub> [35]	14M	✓	75.84	-	-	-	76.04
VinVL <sub>BASE</sub> [91]	5.7M	X	75.95	-	-	-	76.12
VLM <sub>BASE</sub> [77]	4M	X	76.64	-	-	-	76.89
BLIP <sub>BASE</sub> [34]	14M	✓	77.54	-	-	-	77.62
METER-CLIP-ViT <sub>BASE</sub> [13]	4M	X	77.68	92.49	58.07	69.20	77.64
OFA <sub>BASE</sub> [75]	54M	✓	77.98	-	-	-	78.07
SimVLM <sub>BASE</sub> [78]	1.8B	X	77.87	-	-	-	78.14
BLIP <sub>BASE</sub> [34]	129M	✓	78.24	-	-	-	78.17
BLIP <sub>BASE</sub> -CapFilt-L [34]	129M	✓	78.25	-	-	-	78.32
BRIDGE-TOWER <sub>BASE</sub> (Ours)	<b>4M</b>	X	<b>78.66</b>	<b>92.92</b>	<b>60.69</b>	<b>70.51</b>	<b>78.73</b>
BRIDGE-TOWER <sub>BASE</sub> (Ours)	<b>4M</b>	✓	<b>79.10</b>	<b>93.06</b>	<b>62.19</b>	<b>70.69</b>	<b>79.04</b>
UNITER <sub>LARGE</sub> [5]	4M	✓	73.82	-	-	-	74.02
VILLA <sub>LARGE</sub> [16]	4M	✓	74.69	-	-	-	74.87
UNIMO <sub>LARGE</sub> [37]	4M	X	75.06	-	-	-	75.27
VinVL <sub>LARGE</sub> [91]	5.7M	X	76.52	92.04	61.50	66.68	76.63
SimVLM <sub>LARGE</sub> [78]	1.8B	X	79.32	-	-	-	79.56
VLM <sub>LARGE</sub> [77]	4M	X	79.94	-	-	-	79.98
SimVLM <sub>HUGE</sub> [78]	1.8B	X	80.03	93.29	66.54	72.23	80.34
METER-CoSwin <sub>HUGE</sub> [13]	14M	X	80.33	94.25	64.37	72.30	80.54
OFA <sub>LARGE</sub> [75]	54M	✓	80.43	93.32	<b>67.31</b>	72.71	80.67
BRIDGE-TOWER <sub>LARGE</sub> (Ours)	<b>4M</b>	X	<b>81.25</b>	<b>94.69</b>	64.58	<b>73.16</b>	<b>81.15</b>
BRIDGE-TOWER <sub>LARGE</sub> (Ours)	<b>4M</b>	✓	<b>81.52</b>	<b>94.80</b>	66.01	<b>73.45</b>	<b>81.49</b>

Table 5: Comparisons with previous models on visual entailment (SNLI-VE), image retrieval (IR) and text retrieval (TR) tasks (Flickr30K). The best score is **bolded**.

Model	# Pre-train Images	SNLI-VE		Flickr30K (1K test set)						
		dev	test	IR@1	IR@5	IR@10	TR@1	TR@5	TR@10	RSUM
<i>Pre-trained on More Data</i>										
ALIGN <sub>BASE</sub> [27]	1.8B	-	-	84.9	97.4	98.6	95.3	99.8	100.0	576.0
ALBEF <sub>BASE</sub> [35]	14M	80.80	80.91	85.6	97.5	98.9	95.9	99.8	100.0	577.7
<i>Pre-trained on CC, SBU, MSCOCO and VG datasets</i>										
ViLT <sub>BASE</sub> [29]	4M	-	-	64.4	88.7	93.8	83.5	96.7	98.6	525.7
UNITER <sub>LARGE</sub> [5]	4M	79.30	79.38	75.6	94.1	96.8	87.3	98.0	99.2	550.9
VILLA <sub>LARGE</sub> [16]	4M	80.18	80.02	76.3	94.2	96.8	87.9	97.5	98.8	551.5
UNIMO <sub>LARGE</sub> [37]	4M	<b>81.11</b>	80.63	78.0	94.2	97.1	89.4	98.9	99.8	557.5
ALBEF <sub>BASE</sub> [35]	4M	80.14	80.30	82.8	96.7	98.4	94.3	99.4	99.8	571.4
METER-CLIP-ViT <sub>BASE</sub> [13]	4M	80.86	<b>81.19</b>	82.2	96.3	98.4	94.3	99.60	99.9	570.7
BRIDGE-TOWER <sub>BASE</sub> (Ours)	<b>4M</b>	<b>81.11</b>	<b>81.19</b>	<b>85.8</b>	<b>97.6</b>	<b>98.9</b>	<b>94.7</b>	<b>99.61</b>	<b>100.0</b>	<b>576.6</b>

### 4.3 Comparison with Previous Arts

In this section, we describe how we pre-train BRIDGE-TOWER with the best-performing setting (*i.e.*, Add&Norm and  $L_Z = 6$ ) and we compare its fine-tuning performance with previous work.

**Pre-training Setup.** We use four public image-caption datasets for pre-training: Conceptual Captions (CC) [62], SBU Captions [52], MSCOCO Captions [4], and Visual Genome (VG) [31]. The total number of the unique images in the combined training data is 4M. The statistics of these datasets are shown in Appendix. We pre-train BRIDGE-TOWER<sub>BASE</sub> for 100k steps on 64 NVIDIA A100 GPUs with a batch size of 4,096. The learning rate in pre-training is set to  $1e^{-5}$ . No data augmentation is used except for center-crop [13, 55]. The image resolution in pre-training is set to  $288 \times 288$ . Other hyperparameters remain unchanged based on the ablation experiments.

**Main Results.** Table 4 and Table 5 show the performance of BRIDGE-TOWER compared with previous work on downstream VL tasks. With only 4M images for pre-training, BRIDGE-TOWER<sub>BASE</sub> achieves either best or competitive performance on all the downstream tasks, in particular 78.73% accuracy on the VQAv2 test-std set, outperforming the previous state-of-the-art METER model by 1.09% with the same pre-training data and almost negligible additional parameters and computational cost. Remarkably, BRIDGE-TOWER<sub>BASE</sub> not only outperforms all base-size models that use the same number or a higher number of pre-trained images, but it even outperforms some large-size models that use the same number or a higher number of pre-trained images. A similar trend also occurs on the visual entailment and image-text retrieval tasks. On the Flickr30K dataset, BRIDGE-TOWER<sub>BASE</sub> achieves the best performance, outperforming not only ALBEF with its specially designed pre-training targets, but also ALIGN with 1.8B pre-train images.

**Scaling the Model.** To investigate the effect of the scale of the model structure on performance, we replace our uni-modal encoders with the corresponding large version, *i.e.*, RoBERTa<sub>LARGE</sub> with 355M parameters and CLIP-ViT-L/14 with 304M parameters. For each layer of the cross-modal encoder, the hidden size is set to 1,024, the intermediate size of feed-forward networks is set to 4,096, and the number of heads is set to 16. The number of cross-modal encoder layers remains 6 so the number of parameters grows to 200M. The patch size is  $14 \times 14$ , then we set the image resolution to  $294 \times 294$  in pre-training and to  $574 \times 574$  in fine-tuning on the VQAv2. Other hyperparameters remain unchanged. As shown in Table 4, BRIDGE-TOWER outperforms previous models trained with 10 times or even 1,000 times more images, not only in the base size but also in the large size. Notably, BRIDGE-TOWER<sub>LARGE</sub> achieves 81.15% accuracy on the VQAv2 test-std set, surpassing the previous state-of-the-art OFA<sub>LARGE</sub> model by 0.48%. This further demonstrates the effectiveness and scalability of BRIDGE-TOWER. Besides, additional question-answer pairs from Visual Genome can further improve performance on VQAv2 [72, 87]. It can improve our performance to 79.04% and 81.49% on the VQAv2 test-std set in the base and large size, respectively.

## 5 Conclusion and Future Work

We present BRIDGE-TOWER, a simple yet effective vision-language model. BRIDGE-TOWER introduces multiple bridge layers to build a connection between the top layers of uni-modal encoders and each layer of the cross-modal encoder. This enables detailed bottom-up interaction between visual and textual representations at different semantic levels, which promotes more effective cross-modal alignment and fusion in the cross-modal encoder. We experimentally prove the effectiveness of the proposed bridge layers and BRIDGE-TOWER, which achieves remarkable performance in downstream VL tasks without almost no additional parameters and computational cost. We hope that our work will draw more attention to the rich semantic information latent in the different layers of uni-modal encoders. We demonstrate that incorporating this information into cross-modal alignment and fusion can yield more expressive and powerful vision-language representations. Furthermore, in principle, any visual, textual, or cross-modal encoder can be used in the proposed BRIDGE-TOWER architecture.

In the future, we plan to improve BRIDGE-TOWER in the following aspects:

**Different Pre-training Objectives.** We followed METER to directly adopt the masked language modeling (MLM) and image-text matching (ITM) as pre-training objectives. More pre-training objectives, such as image-text contrastive learning (ITC) and masked image modeling (MIM), should be incorporated to investigate their impact on BRIDGE-TOWER.

**Larger Scale Pre-training.** We have pre-trained our model with 4M images both on the BASE and LARGE sizes. BRIDGE-TOWER<sub>LARGE</sub> achieves lower accuracy on the “Number” type questions of VQAv2 than the models pre-trained with more data. We expect to investigate the performance of BRIDGE-TOWER after pre-training on larger-scale image-text data.

**Generative Task.** In this paper, we focus on discriminative tasks. It would be interesting to investigate the impact of the proposed bridge layer on the performance of a visual language generation task, such as image captioning.

## References

- [1] Ankur Bapna, Mia Xu Chen, Orhan Firat, Yuan Cao, and Yonghui Wu. 2018. Training deeper neural machine translation models with transparent attention. In *Proceedings of the 2018 Conference on Empirical Methods in Natural Language Processing*, pages 3028–3033. 3
- [2] Yonatan Belinkov, Nadir Durrani, Fahim Dalvi, Hassan Sajjad, and James Glass. 2017. What do neural machine translation models learn about morphology? In *Proceedings of the 55th Annual Meeting of the Association for Computational Linguistics (Volume 1: Long Papers)*, pages 861–872. 3
- [3] Heng-Jui Chang, Shu-wen Yang, and Hung-yi Lee. 2021. Distilhubert: Speech representation learning by layer-wise distillation of hidden-unit bert. *arXiv preprint arXiv:2110.01900*. 3
- [4] Xinlei Chen, Hao Fang, Tsung-Yi Lin, Ramakrishna Vedantam, Saurabh Gupta, Piotr Dollár, and C Lawrence Zitnick. 2015. Microsoft coco captions: Data collection and evaluation server. *arXiv preprint arXiv:1504.00325*. 8, 19
- [5] Yen-Chun Chen, Linjie Li, Licheng Yu, Ahmed El Kholy, Faisal Ahmed, Zhe Gan, Yu Cheng, and Jingjing Liu. 2020. Uniter: Universal image-text representation learning. In *European conference on computer vision*, pages 104–120. Springer. 1, 2, 6, 8, 19
- [6] Jaemin Cho, Jie Lei, Hao Tan, and Mohit Bansal. 2021. **Unifying vision-and-language tasks via text generation**. In *Proceedings of the 38th International Conference on Machine Learning*, volume 139 of *Proceedings of Machine Learning Research*, pages 1931–1942. PMLR. 2
- [7] Ekin D Cubuk, Barret Zoph, Jonathon Shlens, and Quoc V Le. 2020. Randaugment: Practical automated data augmentation with a reduced search space. In *Proceedings of the IEEE/CVF Conference on Computer Vision and Pattern Recognition Workshops*, pages 702–703. 6
- [8] Yuhao Cui, Zhou Yu, Chunqi Wang, Zhongzhou Zhao, Ji Zhang, Meng Wang, and Jun Yu. 2021. Rosita: Enhancing vision-and-language semantic alignments via cross-and intra-modal knowledge integration. In *Proceedings of the 29th ACM International Conference on Multimedia*, pages 797–806. 2
- [9] Jacob Devlin, Ming-Wei Chang, Kenton Lee, and Kristina Toutanova. 2019. **BERT: Pre-training of deep bidirectional transformers for language understanding**. In *Proceedings of the 2019 Conference of the North American Chapter of the Association for Computational Linguistics: Human Language Technologies, Volume 1 (Long and Short Papers)*, pages 4171–4186, Minneapolis, Minnesota. Association for Computational Linguistics. 3, 4, 6
- [10] Alexey Dosovitskiy, Lucas Beyer, Alexander Kolesnikov, Dirk Weissenborn, Xiaohua Zhai, Thomas Unterthiner, Mostafa Dehghani, Matthias Minderer, Georg Heigold, Sylvain Gelly, et al. 2020. An image is worth 16x16 words: Transformers for image recognition at scale. In *International Conference on Learning Representations*. 1, 2, 3, 4
- [11] Zi-Yi Dou, Zhaopeng Tu, Xing Wang, Shuming Shi, and Tong Zhang. 2018. Exploiting deep representations for neural machine translation. In *Proceedings of the 2018 Conference on Empirical Methods in Natural Language Processing*, pages 4253–4262. 2, 3
- [12] Zi-Yi Dou, Zhaopeng Tu, Xing Wang, Longyue Wang, Shuming Shi, and Tong Zhang. 2019. Dynamic layer aggregation for neural machine translation with routing-by-agreement. In *Proceedings of the AAAI Conference on Artificial Intelligence*, volume 33, pages 86–93. 3
- [13] Zi-Yi Dou, Yichong Xu, Zhe Gan, Jianfeng Wang, Shuohang Wang, Lijuan Wang, Chenguang Zhu, Pengchuan Zhang, Lu Yuan, Nanyun Peng, Zicheng Liu, and Michael Zeng. 2022. **An empirical study of training end-to-end vision-and-language transformers**. *Conference on Computer Vision and Pattern Recognition (CVPR)*. 1, 2, 3, 4, 5, 6, 7, 8, 16, 17, 18, 19
- [14] Chen Du, Yanna Wang, Chunheng Wang, Cunzhao Shi, and Baihua Xiao. 2020. Selective feature connection mechanism: Concatenating multi-layer cnn features with a feature selector. *Pattern Recognition Letters*, 129:108–114. 2
- [15] Yifan Du, Zikang Liu, Junyi Li, and Wayne Xin Zhao. 2022. A survey of vision-language pre-trained models. *arXiv preprint arXiv:2202.10936*. 3
- [16] Zhe Gan, Yen-Chun Chen, Linjie Li, Chen Zhu, Yu Cheng, and Jingjing Liu. 2020. Large-scale adversarial training for vision-and-language representation learning. *Advances in Neural Information Processing Systems*, 33:6616–6628. 8

- [17] Yash Goyal, Tejas Khot, Douglas Summers-Stay, Dhruv Batra, and Devi Parikh. 2017. Making the V in VQA matter: Elevating the role of image understanding in Visual Question Answering. In *Conference on Computer Vision and Pattern Recognition (CVPR)*. 1, 6
- [18] Kazuma Hashimoto, Caiming Xiong, Yoshimasa Tsuruoka, and Richard Socher. 2017. A joint many-task model: Growing a neural network for multiple nlp tasks. In *Proceedings of the 2017 Conference on Empirical Methods in Natural Language Processing*, pages 1923–1933. 3
- [19] Kaiming He, Xiangyu Zhang, Shaoqing Ren, and Jian Sun. 2016. Deep residual learning for image recognition. In *Proceedings of the IEEE conference on computer vision and pattern recognition*, pages 770–778. 3, 5, 7
- [20] Lisa Anne Hendricks, John Mellor, Rosalia Schneider, Jean-Baptiste Alayrac, and Aida Nematzadeh. 2021. Decoupling the role of data, attention, and losses in multimodal transformers. *Transactions of the Association for Computational Linguistics*, 9:570–585. 4
- [21] Sepp Hochreiter and Jürgen Schmidhuber. 1997. Long short-term memory. *Neural computation*, 9(8):1735–1780. 3
- [22] Ronghang Hu and Amanpreet Singh. 2021. Unit: Multimodal multitask learning with a unified transformer. In *Proceedings of the IEEE/CVF International Conference on Computer Vision*, pages 1439–1449. 18
- [23] Gao Huang, Zhuang Liu, Laurens Van Der Maaten, and Kilian Q Weinberger. 2017. Densely connected convolutional networks. In *Proceedings of the IEEE conference on computer vision and pattern recognition*, pages 4700–4708. 2, 3
- [24] Zhicheng Huang, Zhaoyang Zeng, Yupan Huang, Bei Liu, Dongmei Fu, and Jianlong Fu. 2021. Seeing out of the box: End-to-end pre-training for vision-language representation learning. In *Proceedings of the IEEE/CVF Conference on Computer Vision and Pattern Recognition*, pages 12976–12985. 2
- [25] Zhicheng Huang, Zhaoyang Zeng, Bei Liu, Dongmei Fu, and Jianlong Fu. 2020. Pixel-bert: Aligning image pixels with text by deep multi-modal transformers. *arXiv preprint arXiv:2004.00849*. 2
- [26] Ganesh Jawahar, Benoît Sagot, and Djamé Seddah. 2019. **What does BERT learn about the structure of language?** In *Proceedings of the 57th Annual Meeting of the Association for Computational Linguistics*, pages 3651–3657, Florence, Italy. Association for Computational Linguistics. 2, 3
- [27] Chao Jia, Yinfei Yang, Ye Xia, Yi-Ting Chen, Zarana Parekh, Hieu Pham, Quoc Le, Yun-Hsuan Sung, Zhen Li, and Tom Duerig. 2021. Scaling up visual and vision-language representation learning with noisy text supervision. In *International Conference on Machine Learning*, pages 4904–4916. PMLR. 1, 2, 8
- [28] Aishwarya Kamath, Mannat Singh, Yann LeCun, Gabriel Synnaeve, Ishan Misra, and Nicolas Carion. 2021. Mdetr-modulated detection for end-to-end multi-modal understanding. In *Proceedings of the IEEE/CVF International Conference on Computer Vision*, pages 1780–1790. 3
- [29] Wonjae Kim, Bokyung Son, and Ildoo Kim. 2021. Vilt: Vision-and-language transformer without convolution or region supervision. In *International Conference on Machine Learning*, pages 5583–5594. PMLR. 1, 2, 3, 6, 8, 18, 19
- [30] Alexander Kirillov, Ross Girshick, Kaiming He, and Piotr Dollár. 2019. Panoptic feature pyramid networks. In *Proceedings of the IEEE/CVF Conference on Computer Vision and Pattern Recognition*, pages 6399–6408. 3
- [31] Ranjay Krishna, Yuke Zhu, Oliver Groth, Justin Johnson, Kenji Hata, Joshua Kravitz, Stephanie Chen, Yannis Kalantidis, Li-Jia Li, David A Shamma, et al. 2017. Visual genome: Connecting language and vision using crowdsourced dense image annotations. *International journal of computer vision*, 123(1):32–73. 8, 17, 19
- [32] Alex Krizhevsky et al. 2009. Learning multiple layers of features from tiny images. 17
- [33] Gen Li, Nan Duan, Yuejian Fang, Ming Gong, and Daxin Jiang. 2020. Unicoder-vl: A universal encoder for vision and language by cross-modal pre-training. In *Proceedings of the AAAI Conference on Artificial Intelligence*, volume 34, pages 11336–11344. 2
- [34] Junnan Li, Dongxu Li, Caiming Xiong, and Steven Hoi. 2022. Blip: Bootstrapping language-image pre-training for unified vision-language understanding and generation. *arXiv preprint arXiv:2201.12086*. 3, 6, 8

- [35] Junnan Li, Ramprasaath Selvaraju, Akhilesh Gotmare, Shafiq Joty, Caiming Xiong, and Steven Chu Hong Hoi. 2021. Align before fuse: Vision and language representation learning with momentum distillation. *Advances in Neural Information Processing Systems*, 34. 1, 3, 6, 8, 16, 19
- [36] Liunian Harold Li, Mark Yatskar, Da Yin, Cho-Jui Hsieh, and Kai-Wei Chang. 2019. Visualbert: A simple and performant baseline for vision and language. *arXiv preprint arXiv:1908.03557*. 2
- [37] Wei Li, Can Gao, Guocheng Niu, Xinyan Xiao, Hao Liu, Jiachen Liu, Hua Wu, and Haifeng Wang. 2021. Unimo: Towards unified-modal understanding and generation via cross-modal contrastive learning. In *Proceedings of the 59th Annual Meeting of the Association for Computational Linguistics and the 11th International Joint Conference on Natural Language Processing (Volume 1: Long Papers)*, pages 2592–2607. 2, 8, 17, 18
- [38] Wei Li, Can Gao, Guocheng Niu, Xinyan Xiao, Hao Liu, Jiachen Liu, Hua Wu, and Haifeng Wang. 2022. Unimo-2: End-to-end unified vision-language grounded learning. *arXiv preprint arXiv:2203.09067*. 3
- [39] Xiujun Li, Xi Yin, Chunyuan Li, Pengchuan Zhang, Xiaowei Hu, Lei Zhang, Lijuan Wang, Houdong Hu, Li Dong, Furu Wei, et al. 2020. Oscar: Object-semantics aligned pre-training for vision-language tasks. In *European Conference on Computer Vision*, pages 121–137. Springer. 2
- [40] Yanghao Li, Hanzi Mao, Ross Girshick, and Kaiming He. 2022. Exploring plain vision transformer backbones for object detection. *arXiv preprint arXiv:2203.16527*. 7
- [41] Junyang Lin, An Yang, Yichang Zhang, Jie Liu, Jingren Zhou, and Hongxia Yang. 2020. Interbert: Vision-and-language interaction for multi-modal pretraining. *arXiv preprint arXiv:2003.13198*. 2
- [42] Tsung-Yi Lin, Piotr Dollár, Ross Girshick, Kaiming He, Bharath Hariharan, and Serge Belongie. 2017. Feature pyramid networks for object detection. In *Proceedings of the IEEE conference on computer vision and pattern recognition*, pages 2117–2125. 2, 3
- [43] Nelson F Liu, Matt Gardner, Yonatan Belinkov, Matthew E Peters, and Noah A Smith. 2019. Linguistic knowledge and transferability of contextual representations. In *Proceedings of the 2019 Conference of the North American Chapter of the Association for Computational Linguistics: Human Language Technologies, Volume 1 (Long and Short Papers)*, pages 1073–1094. 2, 3
- [44] Wei Liu, Dragomir Anguelov, Dumitru Erhan, Christian Szegedy, Scott Reed, Cheng-Yang Fu, and Alexander C Berg. 2016. Ssd: Single shot multibox detector. In *European conference on computer vision*, pages 21–37. Springer. 3
- [45] Yinhan Liu, Myle Ott, Naman Goyal, Jingfei Du, Mandar Joshi, Danqi Chen, Omer Levy, Mike Lewis, Luke Zettlemoyer, and Veselin Stoyanov. 2019. Roberta: A robustly optimized bert pretraining approach. *arXiv preprint arXiv:1907.11692*. 4, 17
- [46] Yongfei Liu, Chenfei Wu, Shao-yen Tseng, Vasudev Lal, Xuming He, and Nan Duan. 2021. Kd-vlp: Improving end-to-end vision-and-language pretraining with object knowledge distillation. *arXiv preprint arXiv:2109.10504*. 2
- [47] Ilya Loshchilov and Frank Hutter. 2018. Decoupled weight decay regularization. In *International Conference on Learning Representations*. 6
- [48] Jiasen Lu, Dhruv Batra, Devi Parikh, and Stefan Lee. 2019. Vilbert: Pretraining task-agnostic visiolinguistic representations for vision-and-language tasks. *Advances in neural information processing systems*, 32. 1, 2, 3, 4
- [49] Arsha Nagrani, Shan Yang, Anurag Arnab, Aren Jansen, Cordelia Schmid, and Chen Sun. 2021. Attention bottlenecks for multimodal fusion. *Advances in Neural Information Processing Systems*, 34. 3, 4
- [50] Muhammad Muzammal Naseer, Kanchana Ranasinghe, Salman H Khan, Munawar Hayat, Fahad Shahbaz Khan, and Ming-Hsuan Yang. 2021. Intriguing properties of vision transformers. *Advances in Neural Information Processing Systems*, 34. 2, 3
- [51] Minheng Ni, Haoyang Huang, Lin Su, Edward Cui, Taroon Bharti, Lijuan Wang, Dongdong Zhang, and Nan Duan. 2021. M3p: Learning universal representations via multitask multilingual multimodal pre-training. In *Proceedings of the IEEE/CVF Conference on Computer Vision and Pattern Recognition*, pages 3977–3986. 2
- [52] Vicente Ordonez, Girish Kulkarni, and Tamara Berg. 2011. **Im2text: Describing images using 1 million captioned photographs**. In *Advances in Neural Information Processing Systems*, volume 24. Curran Associates, Inc. 8, 19

- [53] Matthew E. Peters, Mark Neumann, Mohit Iyyer, Matt Gardner, Christopher Clark, Kenton Lee, and Luke Zettlemoyer. 2018. **Deep contextualized word representations**. In *Proceedings of the 2018 Conference of the North American Chapter of the Association for Computational Linguistics: Human Language Technologies, Volume 1 (Long Papers)*, pages 2227–2237, New Orleans, Louisiana. Association for Computational Linguistics. [2](#), [3](#)
- [54] Matthew E. Peters, Mark Neumann, Luke Zettlemoyer, and Wen-tau Yih. 2018. **Dissecting contextual word embeddings: Architecture and representation**. In *Proceedings of the 2018 Conference on Empirical Methods in Natural Language Processing*, pages 1499–1509, Brussels, Belgium. Association for Computational Linguistics. [2](#), [3](#)
- [55] Alec Radford, Jong Wook Kim, Chris Hallacy, Aditya Ramesh, Gabriel Goh, Sandhini Agarwal, Girish Sastry, Amanda Askell, Pamela Mishkin, Jack Clark, et al. 2021. Learning transferable visual models from natural language supervision. In *International Conference on Machine Learning*, pages 8748–8763. PMLR. [1](#), [2](#), [4](#), [8](#)
- [56] Alec Radford, Jeffrey Wu, Rewon Child, David Luan, Dario Amodei, Ilya Sutskever, et al. 2019. Language models are unsupervised multitask learners. *OpenAI blog*, 1(8):9. [4](#)
- [57] Maithra Raghu, Thomas Unterthiner, Simon Kornblith, Chiyuan Zhang, and Alexey Dosovitskiy. 2021. Do vision transformers see like convolutional neural networks? *Advances in Neural Information Processing Systems*, 34. [2](#)
- [58] Shaoqing Ren, Kaiming He, Ross Girshick, and Jian Sun. 2015. Faster r-cnn: Towards real-time object detection with region proposal networks. *Advances in neural information processing systems*, 28. [3](#)
- [59] Olaf Ronneberger, Philipp Fischer, and Thomas Brox. 2015. U-net: Convolutional networks for biomedical image segmentation. In *International Conference on Medical image computing and computer-assisted intervention*, pages 234–241. Springer. [3](#)
- [60] Olga Russakovsky, Jia Deng, Hao Su, Jonathan Krause, Sanjeev Satheesh, Sean Ma, Zhiheng Huang, Andrej Karpathy, Aditya Khosla, Michael Bernstein, et al. 2015. Imagenet large scale visual recognition challenge. *International journal of computer vision*, 115(3):211–252. [17](#)
- [61] Rico Sennrich, Barry Haddow, and Alexandra Birch. 2016. **Neural machine translation of rare words with subword units**. In *Proceedings of the 54th Annual Meeting of the Association for Computational Linguistics (Volume 1: Long Papers)*, pages 1715–1725, Berlin, Germany. Association for Computational Linguistics. [4](#)
- [62] Piyush Sharma, Nan Ding, Sebastian Goodman, and Radu Soricut. 2018. **Conceptual captions: A cleaned, hypertexted, image alt-text dataset for automatic image captioning**. In *Proceedings of the 56th Annual Meeting of the Association for Computational Linguistics (Volume 1: Long Papers)*, pages 2556–2565, Melbourne, Australia. Association for Computational Linguistics. [8](#), [19](#)
- [63] Sheng Shen, Liunian Harold Li, Hao Tan, Mohit Bansal, Anna Rohrbach, Kai-Wei Chang, Zhewei Yao, and Kurt Keutzer. 2021. How much can clip benefit vision-and-language tasks? *arXiv preprint arXiv:2107.06383*. [2](#), [4](#)
- [64] Yanyao Shen, Xu Tan, Di He, Tao Qin, and Tie-Yan Liu. 2018. Dense information flow for neural machine translation. In *Proceedings of the 2018 Conference of the North American Chapter of the Association for Computational Linguistics: Human Language Technologies, Volume 1 (Long Papers)*, pages 1294–1303. [2](#), [3](#)
- [65] Damien Sileo. 2021. Visual grounding strategies for text-only natural language processing. In *Proceedings of the Third Workshop on Beyond Vision and LAnguage: inTEgrating Real-world kNowledge (LANTERN)*, pages 19–29. [18](#)
- [66] Amanpreet Singh, Ronghang Hu, Vedanuj Goswami, Guillaume Couairon, Wojciech Galuba, Marcus Rohrbach, and Douwe Kiela. 2021. Flava: A foundational language and vision alignment model. *arXiv preprint arXiv:2112.04482*. [18](#)
- [67] Anders Søgaard and Yoav Goldberg. 2016. **Deep multi-task learning with low level tasks supervised at lower layers**. In *Proceedings of the 54th Annual Meeting of the Association for Computational Linguistics (Volume 2: Short Papers)*, pages 231–235, Berlin, Germany. Association for Computational Linguistics. [3](#)
- [68] Weijie Su, Xizhou Zhu, Yue Cao, Bin Li, Lewei Lu, Furu Wei, and Jifeng Dai. 2019. Vi-bert: Pre-training of generic visual-linguistic representations. In *International Conference on Learning Representations*. [1](#), [2](#)

- [69] Chi Sun, Xipeng Qiu, Yige Xu, and Xuanjing Huang. 2019. How to fine-tune bert for text classification? In *China national conference on Chinese computational linguistics*, pages 194–206. Springer. 2, 3
- [70] Hao Tan and Mohit Bansal. 2019. Lxmert: Learning cross-modality encoder representations from transformers. In *Proceedings of the 2019 Conference on Empirical Methods in Natural Language Processing and the 9th International Joint Conference on Natural Language Processing (EMNLP-IJCNLP)*, pages 5100–5111. 2, 3
- [71] Hao Tan and Mohit Bansal. 2020. Vokenization: Improving language understanding with contextualized, visual-grounded supervision. In *Proceedings of the 2020 Conference on Empirical Methods in Natural Language Processing (EMNLP)*, pages 2066–2080. 17, 18
- [72] Damien Teney, Peter Anderson, Xiaodong He, and Anton Van Den Hengel. 2018. Tips and tricks for visual question answering: Learnings from the 2017 challenge. In *Proceedings of the IEEE conference on computer vision and pattern recognition*, pages 4223–4232. 6, 9, 17
- [73] Ashish Vaswani, Noam Shazeer, Niki Parmar, Jakob Uszkoreit, Llion Jones, Aidan N Gomez, Łukasz Kaiser, and Illia Polosukhin. 2017. Attention is all you need. *Advances in neural information processing systems*, 30. 5
- [74] Alex Wang, Amanpreet Singh, Julian Michael, Felix Hill, Omer Levy, and Samuel R. Bowman. 2019. **GLUE: A multi-task benchmark and analysis platform for natural language understanding**. In *International Conference on Learning Representations*. 17
- [75] Peng Wang, An Yang, Rui Men, Junyang Lin, Shuai Bai, Zhikang Li, Jianxin Ma, Chang Zhou, Jingren Zhou, and Hongxia Yang. 2022. Unifying architectures, tasks, and modalities through a simple sequence-to-sequence learning framework. *arXiv preprint arXiv:2202.03052*. 1, 3, 8, 17, 18
- [76] Qiang Wang, Fuxue Li, Tong Xiao, Yanyang Li, Yinqiao Li, and Jingbo Zhu. 2018. Multi-layer representation fusion for neural machine translation. In *Proceedings of the 27th International Conference on Computational Linguistics*, pages 3015–3026. 2, 3
- [77] Wenhui Wang, Hangbo Bao, Li Dong, and Furu Wei. 2021. Vlmo: Unified vision-language pre-training with mixture-of-modality-experts. *arXiv preprint arXiv:2111.02358*. 3, 8
- [78] Zirui Wang, Jiahui Yu, Adams Wei Yu, Zihang Dai, Yulia Tsvetkov, and Yuan Cao. 2021. Simvlm: Simple visual language model pretraining with weak supervision. *arXiv preprint arXiv:2108.10904*. 1, 3, 8
- [79] Tomer Wullach and Shlomo E Chazan. 2022. Enhancing speech recognition decoding via layer aggregation. *arXiv preprint arXiv:2203.11325*. 3
- [80] Qiaolin Xia, Haoyang Huang, Nan Duan, Dongdong Zhang, Lei Ji, Zhifang Sui, Edward Cui, Taroan Bharti, and Ming Zhou. 2021. Xgpt: Cross-modal generative pre-training for image captioning. In *CCF International Conference on Natural Language Processing and Chinese Computing*, pages 786–797. Springer. 2
- [81] Enze Xie, Wenhai Wang, Zhiding Yu, Anima Anandkumar, Jose M Alvarez, and Ping Luo. 2021. Segformer: Simple and efficient design for semantic segmentation with transformers. *Advances in Neural Information Processing Systems*, 34. 2, 3
- [82] Ning Xie, Farley Lai, Derek Doran, and Asim Kadav. 2019. Visual entailment: A novel task for fine-grained image understanding. *arXiv preprint arXiv:1901.06706*. 1, 6
- [83] Haiyang Xu, Ming Yan, Chenliang Li, Bin Bi, Songfang Huang, Wenming Xiao, and Fei Huang. 2021. E2e-vlp: End-to-end vision-language pre-training enhanced by visual learning. In *Proceedings of the 59th Annual Meeting of the Association for Computational Linguistics and the 11th International Joint Conference on Natural Language Processing (Volume 1: Long Papers)*, pages 503–513. 3
- [84] Hongwei Xue, Yupan Huang, Bei Liu, Houwen Peng, Jianlong Fu, Houqiang Li, and Jiebo Luo. 2021. Probing inter-modality: Visual parsing with self-attention for vision-and-language pre-training. *Advances in Neural Information Processing Systems*, 34. 3
- [85] Peter Young, Alice Lai, Micah Hodosh, and Julia Hockenmaier. 2014. **From image descriptions to visual denotations: New similarity metrics for semantic inference over event descriptions**. *Transactions of the Association for Computational Linguistics*, 2:67–78. 1, 6
- [86] Fisher Yu, Dequan Wang, Evan Shelhamer, and Trevor Darrell. 2018. Deep layer aggregation. In *Proceedings of the IEEE conference on computer vision and pattern recognition*, pages 2403–2412. 2, 3

- [87] Zhou Yu, Jun Yu, Yuhao Cui, Dacheng Tao, and Qi Tian. 2019. Deep modular co-attention networks for visual question answering. In *Proceedings of the IEEE/CVF Conference on Computer Vision and Pattern Recognition (CVPR)*. 9, 17
- [88] Matthew D Zeiler and Rob Fergus. 2014. Visualizing and understanding convolutional networks. In *European conference on computer vision*, pages 818–833. Springer. 2, 3
- [89] Yan Zeng, Xinsong Zhang, and Hang Li. 2021. Multi-grained vision language pre-training: Aligning texts with visual concepts. *arXiv preprint arXiv:2111.08276*. 3
- [90] Xiaohua Zhai, Xiao Wang, Basil Mustafa, Andreas Steiner, Daniel Keysers, Alexander Kolesnikov, and Lucas Beyer. 2021. Lit: Zero-shot transfer with locked-image text tuning. *arXiv preprint arXiv:2111.07991*. 17
- [91] Pengchuan Zhang, Xiujun Li, Xiaowei Hu, Jianwei Yang, Lei Zhang, Lijuan Wang, Yejin Choi, and Jianfeng Gao. 2021. Vinvl: Revisiting visual representations in vision-language models. In *Proceedings of the IEEE/CVF Conference on Computer Vision and Pattern Recognition*, pages 5579–5588. 1, 2, 3, 8
- [92] Sixiao Zheng, Jiachen Lu, Hengshuang Zhao, Xiatian Zhu, Zekun Luo, Yabiao Wang, Yanwei Fu, Jianfeng Feng, Tao Xiang, Philip HS Torr, et al. 2021. Rethinking semantic segmentation from a sequence-to-sequence perspective with transformers. In *Proceedings of the IEEE/CVF conference on computer vision and pattern recognition*, pages 6881–6890. 2, 3
- [93] Luwei Zhou, Hamid Palangi, Lei Zhang, Houdong Hu, Jason Corso, and Jianfeng Gao. 2020. Unified vision-language pre-training for image captioning and vqa. In *Proceedings of the AAAI Conference on Artificial Intelligence*, volume 34, pages 13041–13049. 3
- [94] Yukun Zhu, Ryan Kiros, Rich Zemel, Ruslan Salakhutdinov, Raquel Urtasun, Antonio Torralba, and Sanja Fidler. 2015. Aligning books and movies: Towards story-like visual explanations by watching movies and reading books. In *Proceedings of the IEEE international conference on computer vision*, pages 19–27. 18

## A Appendix

### A.1 Implementation Details of Image-Text Retrieval Task

We follow ALBEF [35] to fine-tune our BRIDGE-TOWER on the image-text retrieval tasks. In training, we jointly optimize with image-text contrastive (ITC) loss and image-text matching (ITM) loss. Two linear projections are added on top of both uni-modal encoders to compute the contrastive similarity of image-text pairs via dot product. Then, following ALBEF [35], instead of randomly sampling negatives for the ITM task, for each image (text) in a mini-batch, we use the contrastive similarity distribution from the ITC task to sample one hard in-batch negative text (image). In inference, we first compute the contrastive similarity for all images and texts, and then take the top-k candidates and calculate their ITM scores for ranking.

### A.2 Detailed Performance Comparison on VQAv2

Table 6: Detailed performance comparisons with METER [13] model on visual question answering (VQAv2) both with and without pre-training. The results in the first block come from METER [13]. \* denotes our reimplementation.

Model	Image Size For Pre-training	# Pre-train Images	Use VG-QA For Fine-tuning	Test-Dev Overall
METER-CLIP-ViT <sub>BASE</sub> w/o fusion	-	-	✗	71.75
METER-CLIP-ViT <sub>BASE</sub> w/ fusion	-	-	✗	72.92
METER-CLIP-ViT <sub>BASE</sub> w/o fusion	224	4M	✗	77.19
METER-CLIP-ViT <sub>BASE</sub> w/ fusion	224	4M	✗	77.06
METER-CLIP-ViT <sub>BASE</sub> w/o fusion *	-	-	✗	74.04
METER-CLIP-ViT <sub>BASE</sub> w/ fusion *	-	-	✗	74.52
BRIDGE-TOWER <sub>BASE</sub>	-	-	✗	75.18
METER-CLIP-ViT <sub>BASE</sub>	288	4M	✗	77.68
BRIDGE-TOWER <sub>BASE</sub>	288	4M	✗	78.66
BRIDGE-TOWER <sub>BASE</sub>	288	4M	✓(COCO-only)	78.77
BRIDGE-TOWER <sub>BASE</sub>	288	4M	✓	79.10
METER-CoSwin <sub>HUGE</sub>	384	14M	✗	80.33
BRIDGE-TOWER <sub>LARGE</sub>	294	4M	✗	81.25
BRIDGE-TOWER <sub>LARGE</sub>	294	4M	✓(COCO-only)	81.32
BRIDGE-TOWER <sub>LARGE</sub>	294	4M	✓	81.52

Table 6 shows the detailed performance comparison with METER [13] on VQAv2. All our experiments use an image resolution of  $576 \times 576$  for fine-tuning.

**Comparison Both With and Without Pre-training.** In the first block, METER shows that the fusion strategy can improve performance by a small margin without pre-training, but it can degrade performance after pre-training. We reimplemented the METER model with and without fusion strategy in the second block, which has been shown in Section 4.2.3 of the paper. We perform grid searches over the learning rates, which may contribute to the better performance (71.75%  $\rightarrow$  74.04%, 72.92%  $\rightarrow$  74.52%) compared to the same setting in METER [13]<sup>2</sup>. Without vision-language pre-training, our base model achieves an accuracy of 75.18% on the VQAv2 test-dev set, which outperforms METER [13] both with and without fusion strategy. With vision-language pre-training, our base model achieves an accuracy of 78.66% on VQAv2, which still surpasses both versions of METER [13]. This demonstrates that through the connection established by multiple bridge layers, our BRIDGE-TOWER achieves comprehensive and detailed layer-wise interaction between the uni-modal representations of different semantic levels.

<sup>2</sup>Besides, the pre-trained checkpoints released in METER’s [github code repository](#) omit the last layer of CLIP-ViT-B/16. [Here](#), they explain that using 11 layers can get slightly better performance (about 0.5% VQA score improvements). However, in our experiments, we don’t find such an improvement and use all the 12 layers for all our base model experiments.

Table 7: Linear probe performance of CLIP-ViT-B/16 on CIFAR-10 and CIFAR-100 before and after VLP.

Model	CIFAR-10	CIFAR-100	AVG
CLIP-ViT-B/16	98.74	90.64	94.69
+ BRIDGE-TOWER Pre-training	98.48	90.20	94.34 (-0.35)
+ METER Pre-training	98.46	89.52	93.99 (-0.70)

Table 8: Fine-tuning performance of RoBERTa<sub>BASE</sub> on GLUE dev sets before and after VLP. The number below each task denotes the number of training examples. BT is short for BRIDGE-TOWER. PT is short for Pre-Training. We report average scores and standard deviations over three runs of different random seeds. Matthews correlations are reported for CoLA, F1 scores are reported for QQP and MRPC, Spearman correlations are reported for STS-B. The average of matched and mismatched accuracy scores are reported for MNLI.

Model	MNLI 392k	QQP 363k	QNLI 108k	SST-2 67k	CoLA 8.5k	STS-B 5.7k	MRPC 3.5k	RTE 2.5k	AVG
RoBERTa <sub>BASE</sub>	87.55±0.03	89.22±0.03	92.87±0.19	95.07±0.30	63.21±2.68	90.70±0.01	92.89±0.35	79.90±0.75	86.43
+ BT PT	87.27±0.02	89.21±0.06	92.78±0.11	94.95±0.11	61.79±0.83	90.85±0.05	92.56±0.61	79.78±0.96	86.15 (-0.28)
+ METER PT	87.25±0.09	89.09±0.07	92.72±0.20	94.65±0.46	61.14±0.45	90.65±0.04	92.12±0.15	79.06±1.08	85.84 (-0.59)

**Utilization of VG-QA for Fine-Tuning.** In the third and fourth blocks, we show the VQAv2 fine-tuning performance of our BRIDGE-TOWER<sub>BASE</sub> model and BRIDGE-TOWER<sub>LARGE</sub> model with different settings of addition question-answer pairs from Visual Genome [31]. Following the standard practice [72, 87], we only use question-answer pairs in Visual Genome where the correct answer appears in the answer classes of VQAv2. We denote the valid 932k question-answer pairs in Visual Genome as VG-QA. In VG-QA, there are 468k question-answer pairs using images that are also used in VQAv2, and we refer to this part of the data as VG-QA(COCO-only). As shown in the last two rows of the third and fourth blocks, VG-QA(COCO-only) can slightly improve the performance of the base model and large model (0.11% and 0.07%, respectively). Using the whole VG-QA can improve our performance to 79.10% and 81.52% on the VQAv2 test-dev set in the base and large size, respectively.

### A.3 Uni-Modal Tasks

Following previous work [13, 37, 71], we report the performance of our visual encoder and textual encoder after vision-language pre-training on uni-modal tasks, to investigate the affect of vision-language pre-training on uni-modal encoders of BRIDGE-TOWER.

For vision tasks, we append a linear classifier to the top of our visual encoder and report the linear probe performance on CIFAR-10 and CIFAR-100 [32]. We perform the grid search over the learning rates and batch sizes for all three models, and the experiments are running on the NVIDIA A100 GPUs. Table 7 shows that, after vision-language pre-training, the performance of our visual encoder drops slightly on both tasks, but still achieves higher performance compared to METER [13], especially on CIFAR-100 (0.68% accuracy improvement). It further proves that the bridge layers of our BRIDGE-TOWER can improve cross-modal interactions while having slighter impediment METER to the intra-modal interactions of the visual encoder compared to METER.

Recently, LiT [90] empirically finds that locked pre-trained image models with unlocked text models work best for vision tasks. They believe that image-text data can be great for learning cross-modal alignment between vision and language, but it may not be precise and clean enough to result in state-of-the-art image encoders. OFA [75] alleviates this problem by adding the image infilling as a pre-training objective, and achieves competitive fine-tuning performance on ImageNet-1K [60]. We will explore the image infilling as a new pre-training objective for BRIDGE-TOWER.

For language tasks, we perform the same grid search as the original RoBERTa<sub>BASE</sub> [45] over the learning rates and batch sizes on the GLUE [74] benchmark. All experiments are running on the NVIDIA V100 GPUs. The best hyperparameters are selected based on the performance over three runs of different random seeds. As shown in Table 8, after vision-language pre-training, the performance of our textual encoder degrades slightly on most of the GLUE tasks (except for the STS-B task). Similar to the results for the vision tasks, our model outperforms METER on all

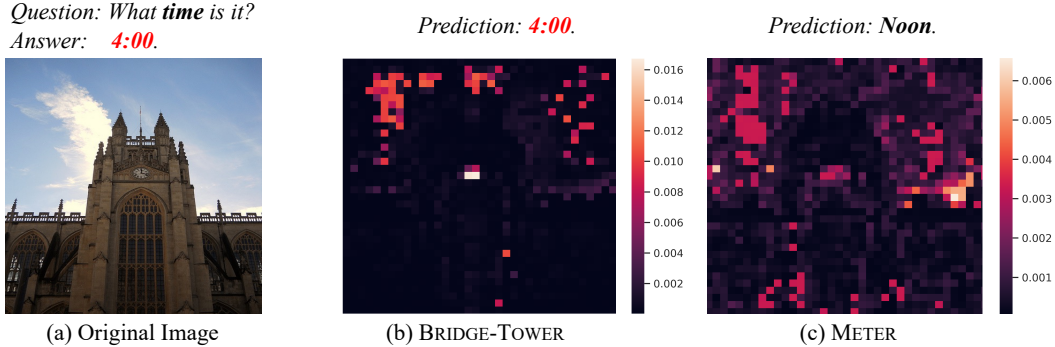


Figure 3: Visualization of the cross-attention map of our BRIDGE-TOWER and METER. The example comes from VQAv2 validation set. Predictions come from the fine-tuning checkpoints of both models.

the GLUE tasks. This demonstrates that our BRIDGE-TOWER almost does not affect intra-modal interactions of the textual encoder.

Besides, the same trend is also observed in many current vision-language models [13, 71], where the performance of the textual encoder decreases slightly after vision-language pre-training. Tan and Bansal [71] shows that the texts in image-caption datasets prefer short and instructive descriptions, and thus cause different distributions of sentence lengths and active words compared to the texts in general text-only corpus, *e.g.*, English Wikipedia and BookCorpus [94]. This contributes to the degradation of the performance after vision-language pre-training. We will jointly explore pre-training on text-only corpus to alleviate this problem [37].

Notably, in both tasks, we only remain the visual or textual encoder in our BRIDGE-TOWER<sub>BASE</sub> model and ignore the cross-modal encoder. Recent works [22, 65, 66, 75] have explored how to utilize the whole vision-language model for uni-modal tasks. We leave this problem as a future direction.

Overall, BRIDGE-TOWER can better maintain the capability of uni-modal encoders on the CIFAR and GLUE benchmarks compared to METER. Furthermore, it is a promising direction to explore more uni-modal pre-training objectives for BRIDGE-TOWER.

#### A.4 Visualization

In this section, we use the heatmap of the attention scores to visualize the difference between our BRIDGE-TOWER and METER. We visualize the cross-attention map from the selected token “**time**” to the image. We use the average attention scores from all attention heads at the last layer of cross-modal encoder. As shown in Figure 3, given the question: “*What time is it?*”, our BRIDGE-TOWER can correctly attend to the clock in the clock tower and the sky in the background and predict the time shown on the clock, while the METER is distracted by the sky in the background. We attribute this to the fact that METER focus on the global information in the last-layer uni-modal features, while our BRIDGE-TOWER can obtain the different semantic levels of visual and textual representations through multiple bridge layers, and interact thoroughly and mildly in the bottom-up directions. Therefore, comprehensive and detailed layer-wise interactions in the cross-model encoder help our BRIDGE-TOWER to predict the time in the clock.

#### A.5 Experimental Settings

Table 9: Statistics of the pre-training datasets. We remove duplicate image-caption pairs in VG [13, 29] and only 2.9M image-caption pairs can be downloaded in CC.

	COCO	VG	CC	SBU
# Images	113K	108K	2.9M	860K
# Captions	567K	4.8M	2.9M	860K

**Pre-training Details** Table 9 shows the statistics of our pre-training datasets. Following previous work [5, 13, 29, 35], we adopt four public image-caption datasets for pre-training, including Conceptual Captions (CC) [62], SBU Captions (SBU) [52], MSCOCO Captions (COCO) [4], and Visual Genome (VG) [31]. The total numbers of the unique images and image-caption pairs in the combined training data are 4M and 9M. Table 10 describes the hyperparameters for pre-training of our BRIDGE-TOWER<sub>BASE</sub> and BRIDGE-TOWER<sub>LARGE</sub> models.

**Hyperparameters for Fine-Tuning Downstream Tasks.** Similar to the image-text matching (ITM) pre-training objective, we pass the final representation of [class] token and [<s>] token to the non-linear layer activated by Tanh, and feed the concatenation of the output into a linear classifier (Flickr30K) or an MLP classifier (VQAv2 and SNLI-VE). We apply cross-entropy loss for SNLI-VE and Flickr30K and binary cross-entropy loss for VQAv2 [13, 29]. Fine-tuning hyperparameters for VQAv2, SNLI-VE, Flickr30K are given in Table 11.

Table 10: Hyperparameters for pre-training BRIDGE-TOWER<sub>BASE</sub> and BRIDGE-TOWER<sub>LARGE</sub>. The first block is the hyperparameters for the cross-modal encoder in our BRIDGE-TOWER model.

Hyperparameters	BRIDGE-TOWER <sub>BASE</sub>	BRIDGE-TOWER <sub>LARGE</sub>
Number of Layers	6	6
Hidden size	768	1,024
FFN inner hidden size	3,072	4,096
Number of Attention heads	12	16
Dropout Ratio	0.1	0.1
Attention dropout	0.1	0.1
Total Steps	100k	100k
Batch Size	4,096	4,096
Optimizer	AdamW	AdamW
Learning Rate	$1e^{-5}$	$1e^{-5}$
Learning Rate Decay	Linear	Linear
Weight Decay	0.01	0.01
Warmup Steps	10k	10k
Adam $\epsilon$	$1e^{-8}$	$1e^{-8}$
Adam $\beta_1$	0.9	0.9
Adam $\beta_2$	0.98	0.98
Center-Crop	✓	✓
Random Resized Crop	✗	✗
Random Augmentation	✗	✗
Random Horizontal Flipping	✗	✗
Textual Encoder	RoBERTa <sub>BASE</sub>	RoBERTa <sub>LARGE</sub>
Visual Encoder	CLIP-ViT-B	CLIP-ViT-L
Patch Size	16	14
Image Resolution	288	294

Table 11: Hyperparameters for fine-tuning BRIDGE-TOWER on downstream VL tasks. CE and BCE are short for cross-entropy loss and binary cross-entropy loss, respectively.

Hyperparameters	VQAv2	SNLI-VE	Flickr30K
Total Epochs	10	5	20
Batch Size	512	64	512
Optimizer	AdamW	AdamW	AdamW
Learning Rate	$1e^{-5} / 4e^{-6}$	$3e^{-6}$	$5e^{-6}$
Learning Rate Decay	Linear	Linear	Linear
Weight Decay	0.05	0.01	0.01
Warmup Ratio	0.06	0.06	0.05
Adam $\epsilon$	$1e^{-8}$	$1e^{-8}$	$1e^{-8}$
Adam $\beta_1$	0.9	0.9	0.9
Adam $\beta_2$	0.98	0.98	0.98
Center-Crop	✗	✗	✗
Random Resized Crop	✓	✓	✓
Random Augmentation	✓	✓	✓
Random Horizontal Flipping	✗	✓	✓
Image Resolution	576 / 574	384	384
Textual Encoder	RoBERTa <sub>BASE/LARGE</sub>	RoBERTa <sub>BASE</sub>	RoBERTa <sub>BASE</sub>
Visual Encoder	CLIP-ViT-B / L	CLIP-ViT-B	CLIP-ViT-B
Patch Size	16 / 14	16	16
Image Resolution	288 / 294	288	288
Loss Function	BCE	CE	CE